International Journal of GEOMATE, Oct., 2021, Vol.21, Issue 86, pp.55-62
ISSN: 2186-2982 (P), 2186-2990 (O), Japan, DOI: https://doi.org/10.21660/2021.86.j2276
Geotechnique, Construction Materials and Environment

SIMULATION OF ROCK CRACK AND PERMEABILITY IN DAM FOUNDATION DURING HYDRAULIC FRACTURING

Thawatchai Chalermpornchai[1], *Bunpoat Kunsuwan[2] and Warakorn Mairaing[3]

[1,2,3] Department of Civil Engineering, Faculty of Engineering at Kamphaeng Saen, Kasetsart University, Thailand

*Corresponding Author, Received: 21 July 2021, Revised: 06 Sept. 2021, Accepted: 23 Sept. 2021

ABSTRACT: Hydraulic fracturing is one type of the dam internal erosion leading to concentrated leaks and dam failure. During reservoir impounding, cracks in rock or soil can be initiated and expanded by water pressure. The crack expansion increases the permeability of the soil or rock foundations. A numerical model of crack deformation was established based on the finite elements method to study crack characteristics due to hydraulic fracturing pressure. The crack of 1 mm wide and 600 mm long is modeled on 1 x 1 m of rock mass with the overburden pressure and pore pressure in the crack. The permeability of crack rock with orientations was examined using the equivalent permeability based on crack width due to hydraulic fracturing. The results revealed that crack closure varied with the elastic modulus of the filler and the orientation along the crack surface. During reservoir impounding, the crack openings were related to hydraulic pressure and crack orientation. The model of crack opening indicated that the vertical crack orientation was likely to widen more than the horizontal crack orientation, with crack openings in the range 0.003-0.37 mm. The range in rock crack permeability with such crack openings was $5x10^{-6}$-1.65 m/s that agreed well with the range of field permeability based on the Lugeon test of $1.27x10^{-4}$ to $4.96x10^{-3}$ m/s. Crack openings due to hydraulic fracturing can be used to predict the rock crack permeability within the hydraulic fracturing area in the dam or its foundation.

Keywords: Crack deformation, Earth dams, Hydraulic fracturing, Rock crack permeability

1. INTRODUCTION

Damages and failure of earth dams due to piping erosion account for 30-50% of total failures [1-3]. The cause is usually concentrated leaks from seepage through the dam and its foundation. Under pressure, the water seeps through expanded cracks in the soil or rock, causing progressive erosion called hydraulic fracturing [4].

Cracks in soil or rock foundation are considered a significant issue for dam safety and they often occur after the first or second reservoir filling. A concentrated leak from the dam and its foundations can lead to breaching failure. Cracks due to hydraulic fracturing are generally induced by the rising water level in the reservoir and the resulting water pressure exceeds the normal stress on pre-existing cracks [5].

Well-known studies on internal erosion by crack expansion mentioned the Teton dam [6] and the Hyttejuvet dam [7]. However, detailed study is still limited on crack expansion related to permeability. Liu *et al.* [8] showed the relationship between crack deformation and permeability in a laboratory triaxial test.

The current paper attempts to research the cracking mechanism due to hydraulic fracturing in a case study of Dike 4 in the Sirikit Dam. Crack deformations were studied using the finite element method (FEM) on various factors such as reservoir level, crack orientations and spacings, rock and crack-filler stiffness. Finally, the crack characteristics were related to rock mass permeabilities. The results will provide the relevant data for further studies of dam leakage due to hydraulic fracturing.

2. BACKGROUND

2.1 Hydraulic Fracturing

Cracks in dams result from many factors, such as differential settlements, seismic activity, and hydraulic fracturing. Leakage through cracks can initiate progressive piping and failure of earth dams. Internal erosion is one of the major failure modes for earth dams, appurtenant structure, and levees.

Failures and incidents by internal erosion of embankment dams and their foundations were classified by the International Commission on Large Dams (ICOLD) into three general failure modes as shown in Fig.1. The process of internal erosion begun with the initiation and continuation of erosion resulting in the progression to form the breach formation for internal erosion and piping. The problem to detect that internal erosion has been initiated relates to the typical processes of initiation: concentrated leak, backward erosion, suffusion, and contact erosion [9].

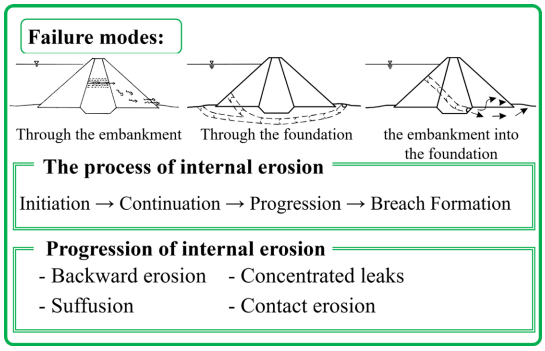

Fig.1 Internal erosion process leading to dam failure

Usually, the concentrated leaks occur on earth dams during the first or second reservoir fillings. The cracks form at the end of just after construction at the location of stress arching [5, 10].

Cracks due to hydraulic fracturing can occur in the dam body or its foundation when the seepage pressure at a particular location is greater than the minor principal stress plus the tensile strength of the soil [9]. Then critical hydraulic fracturing (HF) pressure is given by Eq. (1):

$$U_f = \sigma_3 + T_s \tag{1}$$

where; U_f is the HF pressure; σ_3 is the minor principal stress; and T_s is the tensile strength of the soil or rock. With cracked or cleavage rock, the tensile strength is negligible. In such cases, the critical hydraulic fracturing (HF) pressure is given by Eq. (2).

$$U_f \geq \sigma_3 \tag{2}$$

HF is the progressive process; when seepage pressure from reservoir filling reaches the trigger level, and a crack can propagate from pre-existing cracks. Thus detection and protection of hydraulic fracturing is important for the safety of dams [11].

2.2 Cracking Process Due to Hydraulic Fracturing

In general, pre-existing rock cracks occur as a result of the weathering process on rock joints and bedding [12]. When the dam is impounded, hydraulic pressure causes the expansion of cracks and this can increase permeability and lead to concentrated leakage and dam instability [13].

Existing rock before dam construction contains cracks and filler material in the crack [14]. After the dam construction, the settlement of earth dams is dependent on the influence of deformation moduli and the characteristics of the embankment [15]. The crack width is reduced by the imposed load of the dam. However, the cracks are expanded by the HF pressure during reservoir impounding, as shown in Fig.2.

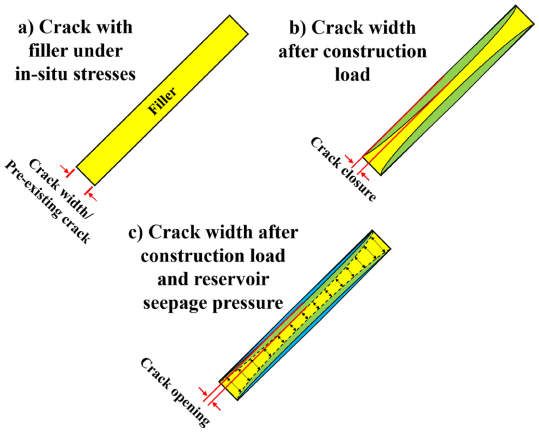

Fig.2 Stages of crack deformation

Stage a) Crack with filler under in-situ stresses: Weathering of the rock and soil by physical and chemical processes can cause cracks. The weathered or transported material can fill in the crack. This stage is pre-existing cracks with filler in the cracks.

Stage b) Crack after construction load: After dam construction, the crack width closes due to embankment loading.

Stage c) Crack after construction load and reservoir seepage pressure: After the first reservoir filling, water pressures penetrate into pre-existing cracks which can re-open the cracks and create hydraulic fracturing erosion.

2.3 Permeability of Rock Mass with Cracks

The rock mass naturally contains fractures and cracks. The cracks may be partially or fully filled with filler materials of rock or small soil particles [16]. The permeability of the rock mass increases according to the crack openings [17].

At present, detailed studies on permeability with a filler in cracks have been conducted modeled using the cubic law by establishing a Darcy-Stokes model as shown in Fig.3. The permeability of a crack (k_c) is expressed as a function of the crack width (w) as shown in Eq. (3) [18, 19].

$$k_c = \frac{gw^2}{12v} \tag{3}$$

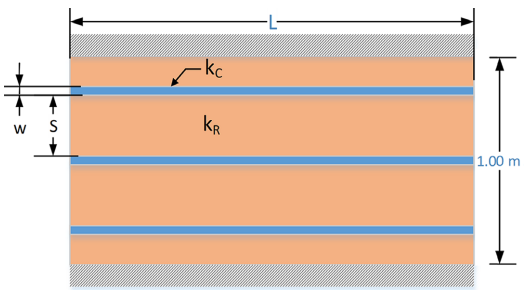

Fig.3 Generalized model of rock mass with cracks

where *g, w,* and *v* are gravitational acceleration, crack width, and kinematic viscosity of the fluid, respectively. Overall permeability of rock mass with cracks or the equivalent permeability (k_T) can be derived as given in Eq. (4).

$$k_T = k_R + n_c \cdot w(k_c - k_R) \quad (4)$$

Where k_R is the permeability of intact rock. n_c is the number of cracks per 1.00 meter of a rock.

2.4 Study Area

The saddle dam (Dike 4) of the Sirikit Hydro-power Dam project was used in the current case study. The dam is located in Tha Pla district, Uttaradit province Thailand. It is an earth dam constructed during 1968 to 1972. Dike 4 is located in the regional geology of metamorphic rock, consisting of phyllite, chlorite-quartz schist, quartzite, quartz schist, and some other metamorphosed rock. The intrusion of igneous rock in the area creates foliation by tectonic forces. Consequently, rock foundations have become overturned folds in the northeast-southwest direction (Fig.4) [20]. The bedding inclination angles are generally 70-90 degrees, measuring from rock cores and outcrops, as shown in Fig.5.

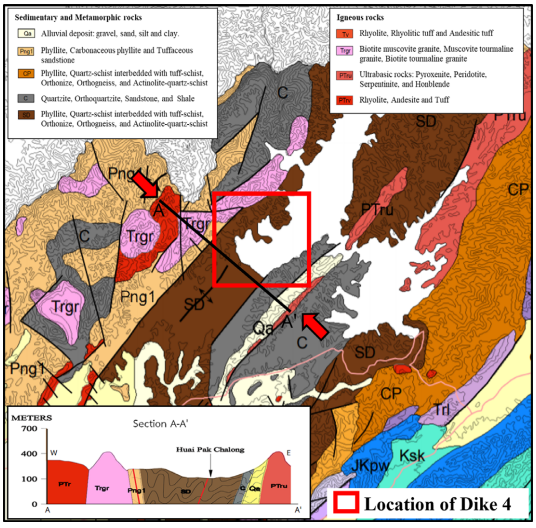

Fig.4 Geology and cross-section of Dike 4 (Modified from DMR, Thailand [21])

During 1995, Dike 4 exhibited problems with seepage and stability on the downstream slope. The wet area was also visible downstream of the dam. Piezometer readings were closely related to the reservoir water level. The high-pressure layer was in the lower part of the residual soil sitting on the highly weathered phyllite. This can cause stress-arching that allows the water to seep through the crack opening.

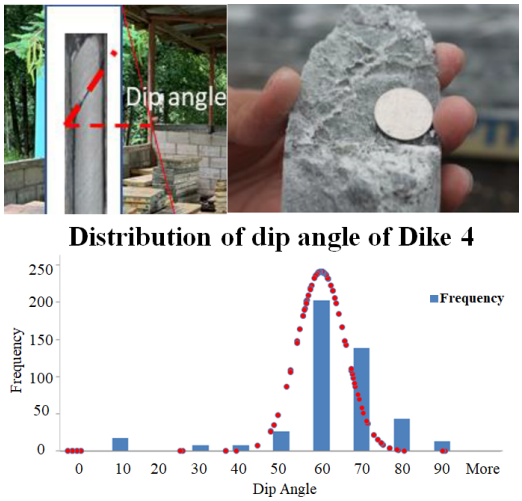

Fig.5 Field measurements from rock cores to assess distribution for dip angle

A Semi-Quantitative Risk Assessment report by the Geotechnical Engineering Research and Development Center [22] indicated that Dike 4 had potential for internal erosion that would significantly affect seepage and the stability of the dam. Thus, the study of crack characteristics due to hydraulic fracturing is essential evidence to explain these phenomena. The current rock crack modeling was performed using the finite element method (FEM).

3. MATERIALS AND METHODS

3.1 Crack Deformation after Dam Constructions

Analyses of crack deformation were established based on the FEM applied to model 1 m^2 using SIGMA/W in the GeoStudio package. The 1 x 1 m of rock mass with several patterns of rock crack orientation was used to simulate the rock conditions in the field.

The in-situ stresses were calculated at a depth of 40 m from the dam crest, corresponding to the phyllite layer. Furthermore, the overall pore pressures were equal to the piezometric measurement in the field. As a result, the principal stresses σ_1 and σ_3 were applied to the model as 800 kPa and 500 kPa, respectively. The boundaries were fixed on the bottom and both vertical sides.

An initial crack was assumed to be 1 mm wide, 600 mm long, and completely filled by the filler. Three filler elastic moduli were assigned as E = 1,000, 10,000, and 100,000 kPa. Crack orientations (α) or dip angles were varied using 10º, 22.5º, 45º, 67.5º, and 90º, respectively as shown in Fig.6.

The mechanical parameters of the model were obtained from a study by the Research Center for Sustainable Infrastructure Engineering [23], as shown in Table 1.

Table 1. Mechanical parameters of rock material model

Parameter	Value
Material model	Phyllite
Elastic moduli, E (kPa)	500000
Poisson's Ratio, υ	0.32
Cohesion, c (kPa)	700
Friction angle, $\emptyset$ (°)	28
Permeability, k (m/s)	$5x10^{-6}$

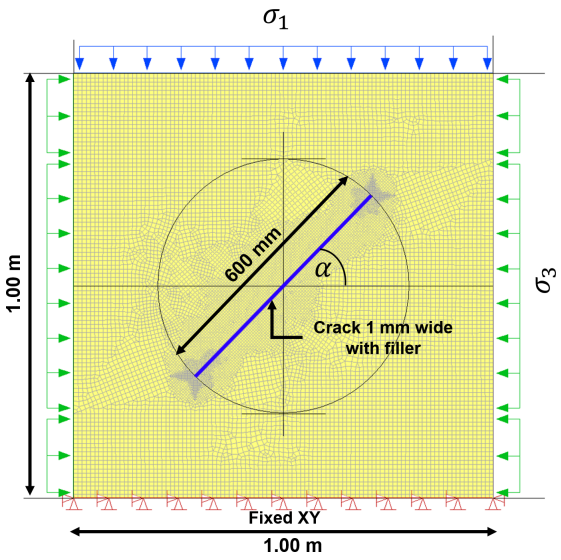

Fig.6 Crack model under in-situ stresses

The filler in the crack model under in-situ stresses was examined based on different crack orientations under different filler elastic moduli to study the factors affecting crack deformation due to the dam construction loading.

3.2 Crack Deformation Due to Hydraulic Fracturing

The first stage of modeling the crack closure due to the construction load was analyzed. Then, the crack expansion from hydraulic fracturing pressure was analyzed. In every case, the minor principal stress and inside water pressure were perpendicular to the crack surfaces [24].

As shown in Fig.7, the left and right boundaries were assigned as fixed in the horizontal direction. Hydraulic pressures in the crack were 50, 100, 150, 200, and 250 kPa, to model possible ranges of seepage pressure from the reservoir. Although there was filler in the crack, the hydraulic pressures were assumed to be fully acting on the crack surface.

The relationship between crack deformation and hydraulic pressures was investigated to estimate the crack opening due to HF pressure with different crack orientations. The crack opening was expressed as crack width due to the HF pressure for later calculation of the rock crack permeability.

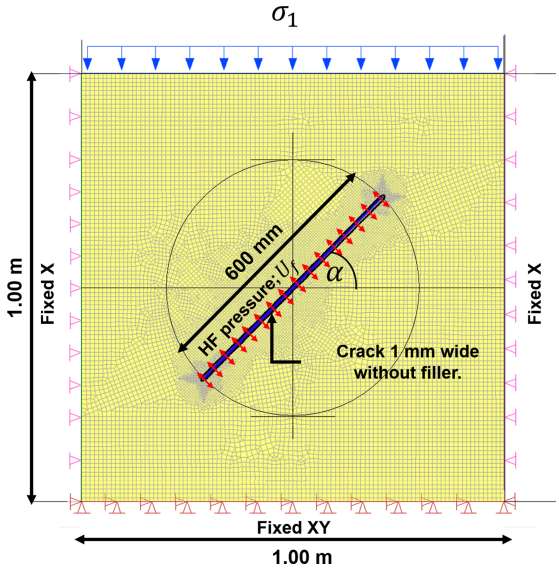

Fig.7 Hydraulic fracturing pressure in crack

3.3 Calculation of Rock Crack Permeability

Rock crack permeability in the dam foundations generally varies with the joint pattern, density, and the degree of weathering. Usually, the seepage water will flow along cracks or joints according to Eq. (3), while flows through intact rock itself are comparatively very small. Thus, the overall permeability of the rock crack is a combination of the intact rock permeability and crack permeability according to Eq. (4), which is called the equivalent permeability.

Permeability is dependent on the joint density and crack/joint spacing, which are obtained from the rock mass rating (RMR). In this study, the joint spacing within a 1 x 1 m of rock mass in the study area based RMR evaluation were mainly in the range 0.01-0.40 m with the depth as shown in Fig.8 and the number of cracks or joints occurring was in the range 1-50 cracks/m [23].

Therefore, the permeability of the rock mass with cracks was investigated based on crack width due to HF pressure and crack spacing to determine the rock crack permeability.

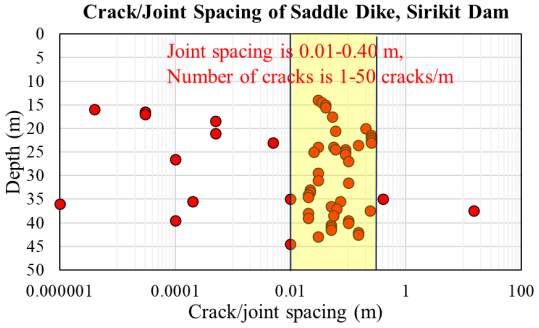

Fig.8 Crack spacing of Saddle Dike, Sirikit Dam

4. RESULTS AND DISCUSSION

4.1 Crack Closure after Dam Construction

The crack deformations of the models were studied for crack orientations of 10º, 22.5º, 45º, 67.5º, and 90º and for filler moduli of 1,000, 10,000, and 100,000 kPa. The crack deformation along the crack surface was established the XY-displacement as the deformation perpendicular to the crack surface. The results for 67.5º crack closure are shown in Fig.9.

This perpendicular displacement along the crack surface varied with the elastic moduli of the filler. Crack closure involves inward crack deformation between the upper and lower locations of the crack surface along the section A-A, as shown in Fig.10.

The surrounding rock is squeezed into a crack by the load from dam construction. The closure for a 67.5^0 crack were 0.4039, 0.0594, and 0.0059 mm for 1,000, 10,000, and 100,000 kPa filler elastic moduli, respectively. Thus, the elastic moduli of the filler had the primary effect on crack closure.

For the crack angles in Fig.11, the crack at $\alpha = 22.5º$ had the maximum crack closure, while the crack at $\alpha = 90º$ had the minimum crack closure. Crack closure for the average bedding angle of $\alpha = 67.5º$ yielded intermediate values.

These analyses illustrated that crack closure increased as the filler elastic modulus decreased. The closure decreased rapidly when the modulus increased from 1,000 to 10,000 kPa but then slowed when the modulus was greater than 10,000 kPa. The crack closure was also dependent on the crack orientation. Even though the filler materials in the crack were assumed to be rather weak materials in the initial stage, when the construction load was applied, the filler would be consolidated and become a denser material later.

4.2 Crack Opening Due to Hydraulic Fracturing

Hydraulic fracturing in the case study was recorded when the reservoir was filled approximately higher than the crack elevation. During the construction, the crack with filler material was squeezed inward to a certain extent. However, in the FEM modeling, the crack surface was subjected to hydraulic fracturing pressure only. The initial crack widths were under zero hydraulic fracturing and were only subjected load from the overburden and dam construction pressure. The initial crack widths before expansion are shown in Table 2.

Table 2 Initial crack width details

Initial crack width, w_i (mm)					
Orientation	10°	22.5°	45°	67.5°	90°
Crack width	0.03	0.18	0.25	0.44	0.49

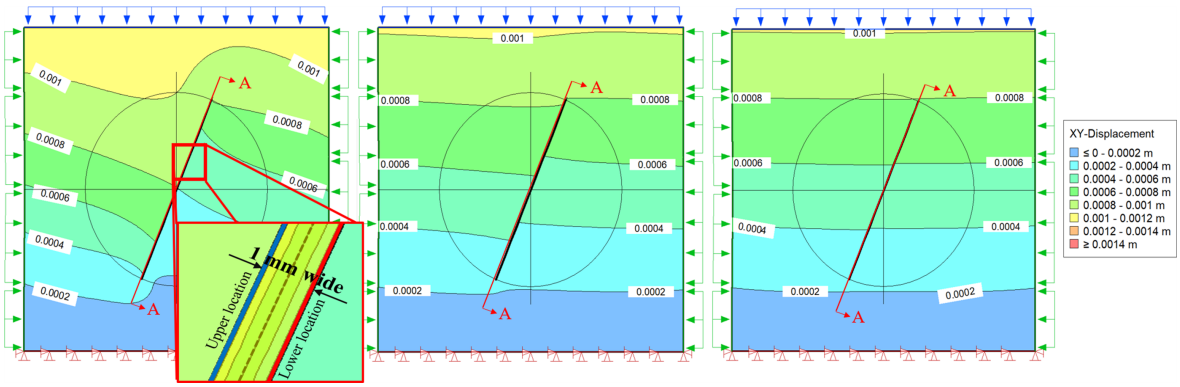

a) $E = 1{,}000$ kPa b) $E = 10{,}000$ kPa c) $E = 100{,}000$ kPa

Fig.9 Crack displacement under construction loading with various filler elastic moduli

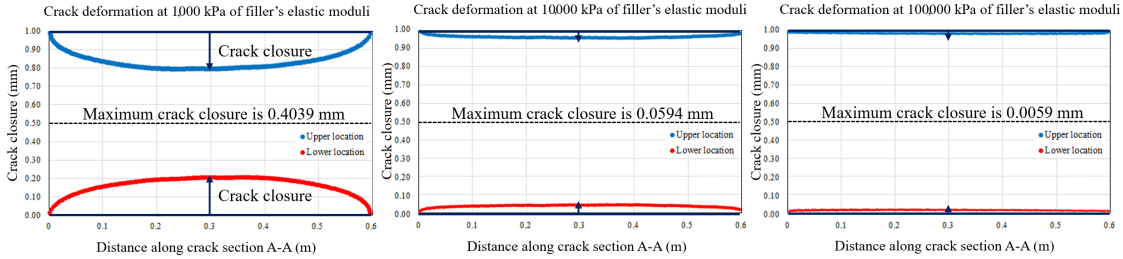

a) $E = 1{,}000$ kPa b) $E = 10{,}000$ kPa c) $E = 100{,}000$ kPa

Fig.10 Crack closure along section A-A with various filler elastic moduli

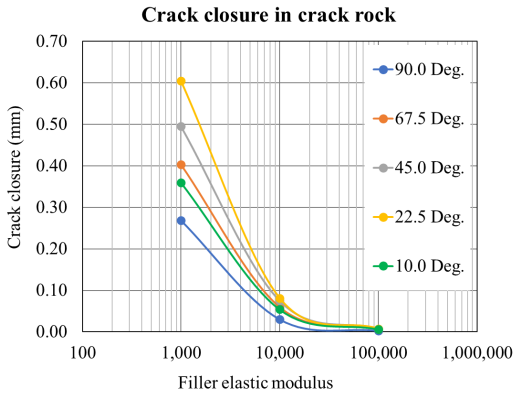

Fig.11 Effect of crack closure based on orientation and filler modulus

Analyses of the crack deformation with orientations under HF pressures were obtained from the XY displacement, as shown for the example of $\alpha = 67.5°$ in Fig.12. The XY displacement along the crack surface was established as the components of deformation perpendicular to crack surface. The crack opening (w_o) due to HF pressure is given by Eq. (5):

$$w_o = \Delta_{XY} - w_i \quad (5)$$

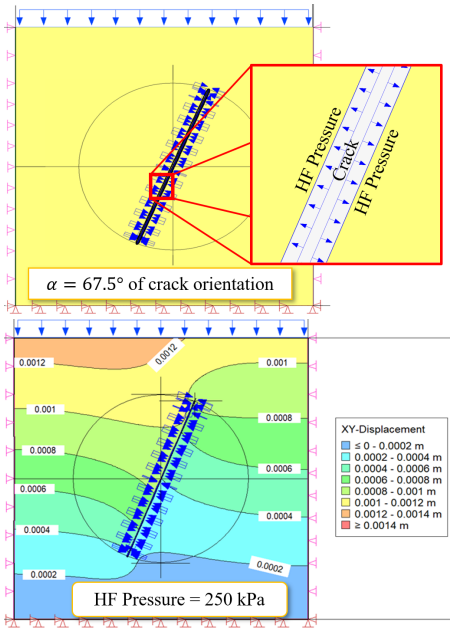

Fig.12 XY displacement of crack due to HF pressure = 250 kPa

where Δ_{XY} is XY displacement perpendicular to the crack plane and w_i is the initial crack width.

Table 3 provides the crack openings under the influence of hydraulic fracturing pressures at various crack orientations.

Fig.13 shows the plot of crack openings at different HF pressures, with the linear relationship between crack opening and HF pressure clearly evident. The crack opening at $\alpha = 90°$ had the highest value of 0.373 mm at 250 kPa pressure. The opening gradually reduced for $\alpha = 67.5°$, 45°, 22.5°, and 10°. The results showed that as the crack angle increased, the crack openings tended to increase. These crack openings were used to calculate the rock mass permeability according to Eq. (3) and (4).

Table 3. Crack openings (mm) under HF pressures

Crack Orientation	Crack Opening, w_o (mm) HF Pressure (kPa) 50	100	150	200	250
10°	0.003	0.008	0.012	0.016	0.020
22.5°	0.027	0.055	0.082	0.109	0.137
45°	0.042	0.084	0.127	0.169	0.211
67.5°	0.066	0.132	0.197	0.263	0.329
90°	0.075	0.149	0.224	0.298	0.373

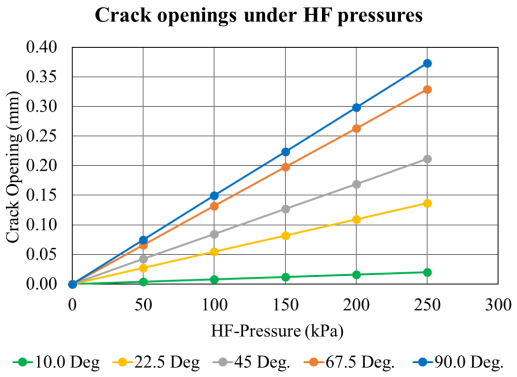

Fig.13 Crack opening under different HF pressures

4.3 Permeability Increasing Due to Hydraulic Fracturing

Fig.14 shows the relationship between rock mass permeability and width of the crack. For one crack per meter of rock, for a width less than 0.0035 mm (the "controlled crack width"), the overall permeability was constant and controlled by the permeability of the intact rock or "intact rock control". For a crack width greater than 0.0035 mm, the overall permeability increased with increasing crack width or "rock crack control". As the number of cracks per meter of rock increased, the controlled crack widths decreased. The controlled crack widths reduced to 0.0015 and 0.0005 mm for 5 and 50 cracks per meter, respectively. These results were in agreement with the rock crack permeability characteristics reported in the studies by Zhang [25] and Ye *et al.* [26].

From the field investigation data as shown in Fig.8, that the number of cracks per meter was commonly in the range 1-50 cracks/m. Overall

permeabilities with the numbers of cracks are expressed in Fig.15 as the relationship between rock permeability and crack width. The maximum controlled crack width was 0.0085 m.

The maximum crack openings for every crack orientation due to hydraulic fracturing were in the range 0.003-0.373 mm and this was defined as the crack width for calculating rock crack permeability. Thus, the range in rock crack permeability was $5x10^{-6}$-1.65 m/s.

This permeability range was covered and matched well with the range of field permeability value from the Lugeon test, which were in the range $1.27x10^{-4}$-$4.96x10^{-3}$ m/s. Thus, the ranges of rock crack permeability calculation and field permeability were in agreement.

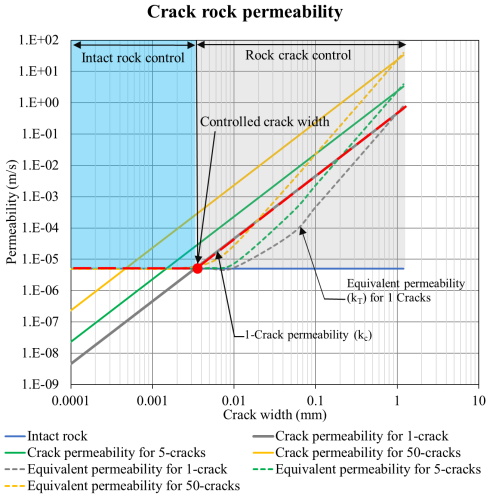

Fig.14 Permeability of intact rock and rock cracks

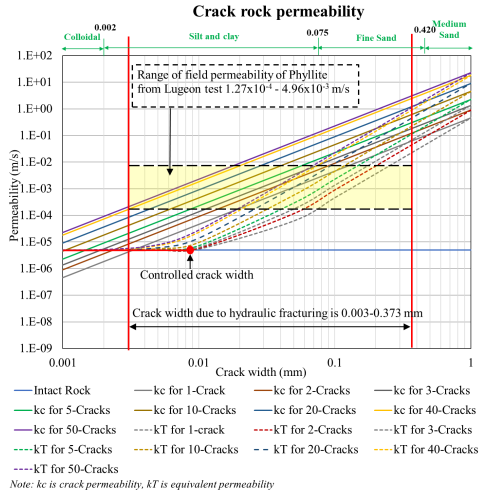

Fig.15 Rock crack permeability and crack width

5. CONCLUSIONS

A numerical model was developed using the finite element method based on a 1 m^2 piece of rock to understand the mechanics of rock cracking. Furthermore, crack closure after dam constructions and crack opening due to hydraulic fracturing were investigated based on crack characteristics.

Rock crack permeability due to hydraulic fracturing was related to crack width based on the crack model. According to the above study, the following conclusions were made.

(1) Our understanding of crack mechanisms can be enhanced using rock crack modelling of crack closure after dam construction and of crack opening due to hydraulic fracturing, with the final crack width related to permeability increasing.

(2) Crack closure increases as the elastic modulus of the filler decreases. A crack at $\alpha = 90^o$ produced the minimum crack closure, while a crack at $\alpha = 22.50^o$ produced the maximum closure. These results suggested that crack closure after dam construction can have a significant impact the variation in the elastic modulus of the filler and the orientation along the crack surface.

(3) A crack at $\alpha = 90^o$ produced the maximum crack opening due to hydraulic fracturing pressures but the opening decreased as the crack angle decreased. The crack opening linearly increased with HF pressure. These findings suggested that a crack opening for a vertical crack orientation would likely be wider than a horizontal crack orientation.

(4) A consequence of crack opening being related to permeability indicated 2 characteristics: intact rock-controlled and rock crack-controlled permeability. The permeability increase was subject to the number of cracks and crack openings.

(5) The results from the modeling of crack openings produced crack widths in the range 0.003-0.37 mm. These crack widths established permeability due to hydraulic fracturing. Thus, the range of rock crack permeability was $5x10^{-6}$-1.65 m/s. This range matched well with the field permeability from the Lugeon test in the field, which was in the range $1.27x10^{-4}$-$4.96x10^{-3}$ m/s.

The results from the model will help to understand crack characteristics. Cracks opening due to hydraulic fracturing can be used to predict the possible range of rock crack permeability.

6. ACKNOWLEDGMENTS

This research was partially supported by a grant from the Faculty of Engineering at Kamphaeng Saen, Kasetsart University, Thailand. The authors appreciate the Graduate Program Scholarship provided by the Department of Civil Engineering, Faculty of Engineering at Kamphaeng Saen, Kasetsart University, Thailand. The authors express special thanks to the Electricity Generating Authority of Thailand for the permission and providing the data for the case study.

7. REFERENCES

[1] ICOLD, Dam Failures Statistical Analysis. 1995.

[2] Foster, M., Fell, R., and Spannagle, M., The statistics of embankment dam failures and accidents. Canadian Geotechnical Journal, 2000. 37(5): p. 1000-1024.

[3] Fell, R., Foster, M., Cyganiewicz, J., Sills, G., Vroman, N., and Davidson, R., Risk Analysis for Dam Safety: A Unified Method for Estimating Probabilities of Failure of Embankment Dams by Internal erosion and Piping Guidance Document. 2008.

[4] Sherard, J.L., Embankment Dam Cracking. Embankment-Dam Engineering, Casagrande Volume., 1973. John Wiley and Sons, New York: p. 271-353.

[5] Wang, J.-J., Hydraulic fracturing in earth-rock fill dams. 2014: John Wiley & Sons.

[6] Seed, H., Leps, T., Duncan, J., and Bieber, R., Hydraulic fracturing and its possible role in the Teton Dam failure. 1976: Failure of Teton dam Report to US Dept. of Interior and State of Idaho.

[7] Kjaernsli, B. and Torblaa, I., Leakage through horizontal cracks in the core of Hyttejuvet Dam. Norwegian Geotechnical Institute Publication, 1968: p. pp. 39-47.

[8] Liu, X., Zhu, Z., and Liu, A., Permeability Characteristic and Failure Behavior of Filled Cracked Rock in the Triaxial Seepage Experiment. Advances in Civil Engineering, 2019.

[9] Fell, R., MacGregor, P., Stapledon, D., Bell, G., and Foster, M., Geotechnical engineering of Dams, 2nd Edition. 2015: CRC press.

[10] Vallejo, L., Shear stresses and the hydraulic fracturing of earth dam soils. Soils and Foundations, 1993. 33(3): p. 14-27.

[11] Tran, D.Q., Nishimura, S., Senge, M., and Nishiyama, T., Research on Cause of Dam Failure from Viewpoint of Hydraulic Fracturing – Case Study of A Dam Failure in Vietnam. International Journal of GEOMATE, 2018. 14(41): p. 86-94.

[12] Arikan, F. and Aydin, N., Influence of weathering on the engineering properties of dacites in Northeastern Turkey. International Scholarly Research Notices, 2012.

[13] Zhu, Z., Niu, Z., Que, X., Liu, C., He, Y., and Xie, X., Study on Permeability Characteristics of Rocks with Filling Fractures Under Coupled Stress and Seepage Fields. Water, 2020. 12(10): p. 2782.

[14] Zhuang, X., Chun, J., and Zhu, H., A comparative study on unfilled and filled crack propagation for rock-like brittle material. Theoretical Applied Fracture Mechanics, 2014. 72: p. 110-120.

[15] Nadia, S. and Bouchrit, R., Influence of deformation moduli on the settlement of earth dams. International Journal of GEOMATE, 2017. 13(38): p. 16-22.

[16] Nhan, P.T., Xi, X., and Suresh, S., Behaviors of crack propagation of rock-like material with different jointed thickness. International Journal of GEOMATE, 2019. 16(58): p. 203-210.

[17] Min, K.-B., Rutqvist, J., Tsang, C.-F., and Jing, L., Stress-dependent permeability of fractured rock masses: a numerical study. International Journal of Rock Mechanics Mining Sciences, 2004. 41(7): p. 1191-1210.

[18] Snow, D.T., A parallel plate model of fractured permeable media. 1965, University of California.

[19] Witherspoon, P.A., Wang, J.S., Iwai, K., and Gale, J.E.J.W.r.r., Validity of cubic law for fluid flow in a deformable rock fracture. 1980. 16(6): p. 1016-1024.

[20] Singharajwarapan, S. and Berry, R.F., Structural analysis of the accretionary complex in Sirikit Dam area, Uttaradit, Northern Thailand. Journal of Southeast Asian Earth Sciences, 1993. 8(1-4): p. 233-245.

[21] Department of Mineral Resources, Geological Map of Uttaradit. 2007: Thailand.

[22] Geotechnical Engineering Research and Development Center, Semi-Quantitative Risk Assessment on Stability of Saddle Dikes of Sirikit Dam. 2019, Electricity Generating Authority of Thailand: Final Report. March, 2019.

[23] Research Center for Sustainable Infrastructure Engineering, Development of Diagnosis Expert System for Seepage through Medium Scale Dam Foundation: Case Study Sirikit Saddle Dam. 2020, Electricity Generating Authority of Thailand: 2nd Progress Report. July, 2020.

[24] Murdoch, L., Forms of hydraulic fractures created during a field test in overconsolidated glacial drift. Quarterly Journal of Engineering Geology and Hydrogeology, 1995. 28(1): p. 23-35.

[25] Zhang, L., Engineering properties of rocks. 2016: Butterworth-Heinemann.

[26] Ye, F., Duan, J.C., Fu, W.X., and Yuan, X.Y., Permeability properties of jointed rock with periodic partially filled fractures. Geofluids, 2019.